Brazilian Journal of Physics (2025) 55:178
https://doi.org/10.1007/s13538-025-01814-w

Analysis of Physicochemical Properties Exhibited by Thermotropic Liquid Crystalline Binary Mixtures

J. Vivekanandan[1,2] · N. Pongali Sathya Prabu[3] · Sang Yeol Lee[1,2]

Received: 1 April 2025 / Accepted: 28 May 2025

Abstract
Five binary mixtures are obtained as the resultant liquid crystalline complexes obtained from the liquid crystal precursors formed between α-Keto Glutaric acid (KGA) with hexyloxy benzoic acid (6BAO) and α-keto glutaric acid (KGA) with dodecyloxy benzoic acid (12BAO). Variation in the molar proportion of the precursors in a well-defined odd step leads to the formation of five liquid crystalline binary mixtures. Rich-phase polymorphism exhibited by the precursors has triggered this analysis which leads to a wide range of results obtained completely investigated by means of spectral, optical, and thermal characterization techniques. Surface morphology investigation confirms the uniformity in obtaining the binary mixture. KGA + 6BAO exhibit smectic C and smectic G mesophases whereas KGA + 12BAO exhibit nematic, smectic C, and smectic G mesophases. Chemical analysis confirming the intermolecular hydrogen bonding is carried through Fourier transform infrared spectroscopy analysis. Optical analysis corresponding to the mesophase variance of the binary mixtures is carried through polarizing optical microscope. Thermal analysis confirming the transition temperatures and enthalpy values is carried out by differential scanning calorimeter.

Keywords Liquid crystalline binary mixtures · Mesophase · Physico-chemical properties · Thermal investigations

1 Introduction

Liquid crystals (LCs) are utilized as the prime component in various applications such as sensors, modulators, solar cells, and display devices [1]. The self-assembling structures with anisotropic nature, technological importance, and the molecular response for the applied external field [2–4] have made these substances, in particular hydrogen bond liquid crystals (HBLCs), a remarkable advanced technological utility. Mesophases and the physicochemical properties possessed by them determine the nature of applicational viability. Many techniques have been adopted by the research [5–7] and have succeeded in obtaining the above statement. The formation of the mixtures between two mesogenic complexes exhibiting rich phase polymorphism is one of the successful methods followed by the scientists [8–15]. The phase separation and self-assembling nature of the binary mixtures obtained provide added functionality of ionic conductivity to these materials [16]. Nematic, the least ordered and sticky among the numerous mesophases, can be readjusted under external stimulation more easily as compared with other mesophases [17]. These materials have found applications in ion transport [17], smart windows [18], reverse-mode PDLCs, [19, 20] etc. The organic crystals exhibit excellent second-order optical nonlinearities that are suitable for a variety of applications, including data processing, ultrafast response, frequency conversion, telecommunications, electro-optics, data storage [21], laser radiation generation, and optical limiters etc. [22]. Co-crystals are an excellent way to improve the physicochemical properties of active pharmaceutical ingredients (API) without changing their pharmacological qualities [23–25]. For the applicational

✉ N. Pongali Sathya Prabu
pongalispn@bitsathy.ac.in

✉ Sang Yeol Lee
sylee2020@gachon.ac.kr

[1] Department of Semiconductor and Electronic Engineering, Gachon University, Seongnam-si, Gyeonggi-do 13120, Republic of Korea

[2] Gachon Advanced Institute of Semiconductor Technology, Gachon University, Seongnam-Si, Gyeonggi 13120, Republic of Korea

[3] Liquid Crystal Research Laboratory (LCRL), Department of Physics, Centre for Research, Bannari Amman Institute of Technology, Sathyamangalam 638 401, India

Published online: 05 June 2025

aspect, the thermal range of mesogenic phases and their associated parameters, the stability of thermal and transitional order can be fine-tuned to the preferred parameters. The development of binary mixtures of liquid crystalline complexes is the traditional method that satisfies the above-stated factors that outfit the liquid crystalline complexes for applicational effectiveness [26–30]. The two-liquid crystalline complex (say X and Y) mixture in the different molar proportions makes the formation of binary mixtures. The binary mixtures of liquid crystalline complexes subjected to electrical, structural, optical, chemical, and thermal properties certainly reveal the essential properties possessed by the prepared binary mixtures [31]. The modification in the molar proportion defines the properties possessed. Hence, choosing the right proportion regulates the efficacy of the mesophases possessed by the binary mixtures.

The current investigation explores the chemical, optical, and thermal properties of the binary mixtures formed between α-ketoglutaric acid (KGA) and p-*n*-alkyloxy benzoic acids (*n*BAO, where *n* represents carbon number; here, it is hexyloxy [6BAO] and dodecyloxy [12BAO] benzoic acids). Odd molar proportion variation in the above two benzoic acids is prepared for the present investigation. Rich-phase polymorphism exhibited by the precursors has triggered this analysis, which leads to a wide range of results obtained that completely investigates the physical and chemical properties possessed by them.

2 Experimental

The physical and chemical properties of the liquid crystalline binary mixtures prepared are investigated by numerous techniques in order to understand the mesogenic changes that are observed during the formation of the binary mixtures. Consistency in the formation of the binary mixtures is confirmed by surface morphological studies carried out using a field emission scanning electron microscope (FESEM) — Carl Zeiss (Sigma-300). Chemical investigations are performed using an ABB Bomem MB 3000 series Fourier transform infrared spectrometer (FTIR) in order to establish the intermolecular hydrogen bonding that exists between the binary mixtures prepared. Optical investigations are carried out through a Nikon Polarizing Optical Microscope (POM) interfaced with Nikon Imagine Software (NIS), which records and retrieves the mesophases exhibited by the binary mixtures. The nature of the mesophase, the onset and offset temperatures of the mesophases, is clearly distinguished from the optical analysis. Thermal investigations are carried out with the aid of a differential scanning calorimeter (DSC) equipped with TA60 software, which details the thermogram of the binary mixtures. Phase transition temperatures, their internal energy involved during endothermic and exothermic processes, mesophase stability, order of transition, and specific heat capacity values are all derived from the thermogram data obtained for the binary mixtures. Chemicals utilized in preparing binary mixtures, viz., α-ketoglutaric acid (KGA), p-*n*-alkyloxy benzoic acids (nBAO, here *n* represents the hexyloxy benzoic acid and dodecyloxy benzoic acid), and the solvent dimethyl formamide (DMF), are of high-performance liquid chromatography (HPLC) grade.

2.1 Preparation of Binary Mixtures

A well-established synthetic route is followed [32] in preparing the liquid crystalline precursors, where 1 mol of α-ketoglutaric acid (KGA) is mixed with 2 mol of p-*n*-alkyloxy benzoic acids (nBAO) in excess DMF, and the resultant liquid crystalline precursor is obtained as the final product. The detailed scheme of synthesis and the molecular representation are reported earlier [31]. In this investigation, two precursors of the existing liquid crystalline complexes are chosen for analysis. α-Ketoglutaric acid (KGA) with hexyloxy benzoic acid (6BAO), abbreviated as KGA + 6BAO, and α-ketoglutaric acid (KGA) with dodecyloxy benzoic acid (12BAO) abbreviated as KGA + 12BAO are the precursors taken for investigation. KGA + 6BAO exhibits smectic C and smectic G mesophases whereas KGA + 12BAO exhibit nematic, smectic C, and smectic G mesophases. The growth/suppression of the mesophases with the variation in the odd molar ratio of the binary mixtures, α-ketoglutaric acid (KGA) with hexyloxy benzoic acid (6BAO), is considered as *X* combination, while α-ketoglutaric acid (KGA) with dodecyloxy benzoic acid (12BAO) is considered as *Y* combination. Variation in the physical and chemical properties is detailed in this present investigation.

3 Results and Discussion

On varying the molar proportions of KGA + 6BAO and KGA + 12BAO in odd steps of 0.1 to 0.9, five binary mixtures are obtained. The products obtained are subjected to repetitive scans in order to well establish the chemical and thermal stability of the mixtures formed [33–35]. The phase variance of the binary mixtures, along with the enthalpy values observed in both heating and cooling cycles, is portrayed in Table 1. The correlation of POM and DSC data reveals the stability of the prepared mixtures.

3.1 Surface Morphology: FESEM

Field emission scanning electron microscope (FESEM)—Carl Zeiss (Sigma-300) provides the information about the surface morphology of the prepared binary mixtures.

Table 1 DSC and POM data obtained for KGA + 6BAO and KGA + 12BAO binary mixtures

Binaries KGA + 6BAO (X) and KGA + 12BAO(Y)	Phase variance	DSC	Crystal to melt	N	C	G	Crystal
0.1X:0.9Y	NCG	H	93.8 (57.92)	135 (2.96)	127.6 (5.03)	[a]	
		C		132.4 (3.54)	128.5 (5.98)	119.4 (2.24)	70.3 (18.77)
		POM		132.9	128.9	119.7	70.5
0.3X:0.7Y	NCG	H	66.7 (20.75)	137.4 (4.29)	116.3 (0.34)	103.4 (1.75)	
		C		132.1 (17.55)	126.3 (4.34)	81.4 (2.94)	55.2 (10.62)
		POM		132.6	126.7	81.6	55.3
0.5X:0.5Y	NC	H	63.24 (19.73)	132.4 (5.40)	[a]		
		C		132.7 (1.51)	126 (4.79)		54.7 (14.11)
		POM		133.2	126.4		55.1
0.7X:0.3Y	NC	H	61.4 (8.34)	141.2 (6.28)	[a]		
		C		146.6 (4.33)	133.3 (6.56)		54.2 (4.49)
		POM		147.1	133.8		54.6
0.9X:0.1Y	NC	H	102.7 (31.66)	145.1 (9.79)	[a]		
		C		140.5 (8.28)	135.3 (10.42)		87.5 (33.61)
		POM		141.1	135.8		87.7

[a]Monotropic transition, enthalpy values (J g^{-1}) given in parenthesis

Figure 1 represents the FESEM images obtained for the precursors KGA + 6BAO, KGA + 12 BAO, and the binary mixture KGA + 6BAO and KGA + 12 BAO (0.1 *X*:0.9 *Y*) respectively. Figure 1 **a** reflects the regularity in the formation of precursor KGA + 6BAO as the molecules are combined uniformly and form a sheet-like structure. Similarly, Fig. 1**b** exhibits the rod-like feature obtained for the precursor KGA + 12BAO, which is also a clear indication of the perfection in obtaining the liquid crystalline complex. As a representative case, Fig. 1**c** portrays the morphology of binary mixtures KGA + 6BAO and KGA + 12 BAO (0.1 *X*:0.9 *Y*) obtained exhibiting the combination of sheet- and rod-like structures in a uniform manner, which is a token of evidence for the binary mixtures prepared to exhibit uniform optical and thermal properties. The same morphology has been noticed in the remaining binary mixtures also.

3.2 Phase Variance Analysis: POM

The phase variance of the binary mixtures prepared is confirmed through POM. Textural observations are made meticulously to confirm the nature of the mesophases and their sequence observed in the five binary mixtures formed. The onset and offset transition temperatures of the mesophase, along with the nature of the mesophase, are clearly noticed from the POM data. Three mesophases, namely, nematic, smectic C, and smectic G, are observed in the present analysis. Confirmation of the mesophase is carried out by comparing the mesophase observed with respect to the Gray and Goodbye textures [36]. Figure 2 **a** shows the fully grown nematic phase, Fig. 2**b** portrays the broken focal conic texture of the smectic C phase, and Fig. 2**c** depicts the multi-colored smooth mosaic texture of the smectic G phase observed.

3.3 Intermolecular Hydrogen Bond Confirmation: FTIR

Confirmation of intermolecular complementary hydrogen bonding and the formation of mesogenic complex upon complexation is the fundamental chemical characterization that needs to be carried out for the hydrogen bond liquid crystals (HBLCs). As the precursors formed are HBLC, the binary mixtures formed between two HBLCs will also be HBLC binary mixtures. This argument is well proved from the chemical investigation undertaken with the aid of an FTIR spectrometer. The binary mixtures are well powdered, grinded, and blended with FTIR-grade potassium bromide (KBr), and the pellets obtained are exposed to the mid-IR range for the spectra. Table 2 reflects the hydrogen bond formation and the mesogenic complex confirmation for all five binary mixtures prepared. As a representative case, the FTIR spectrum of KGA + 6BAO and KGA + 12 BAO (0.1 *X*/0.9 *Y*) is shown as Fig. 3. Two sharp peaks noticed at 2923 cm^{-1} and 1689 cm^{-1} confirm the objective of the chemical analysis. The magnitudes of the functional groups obtained are in good accordance with the reported literature [37–40].

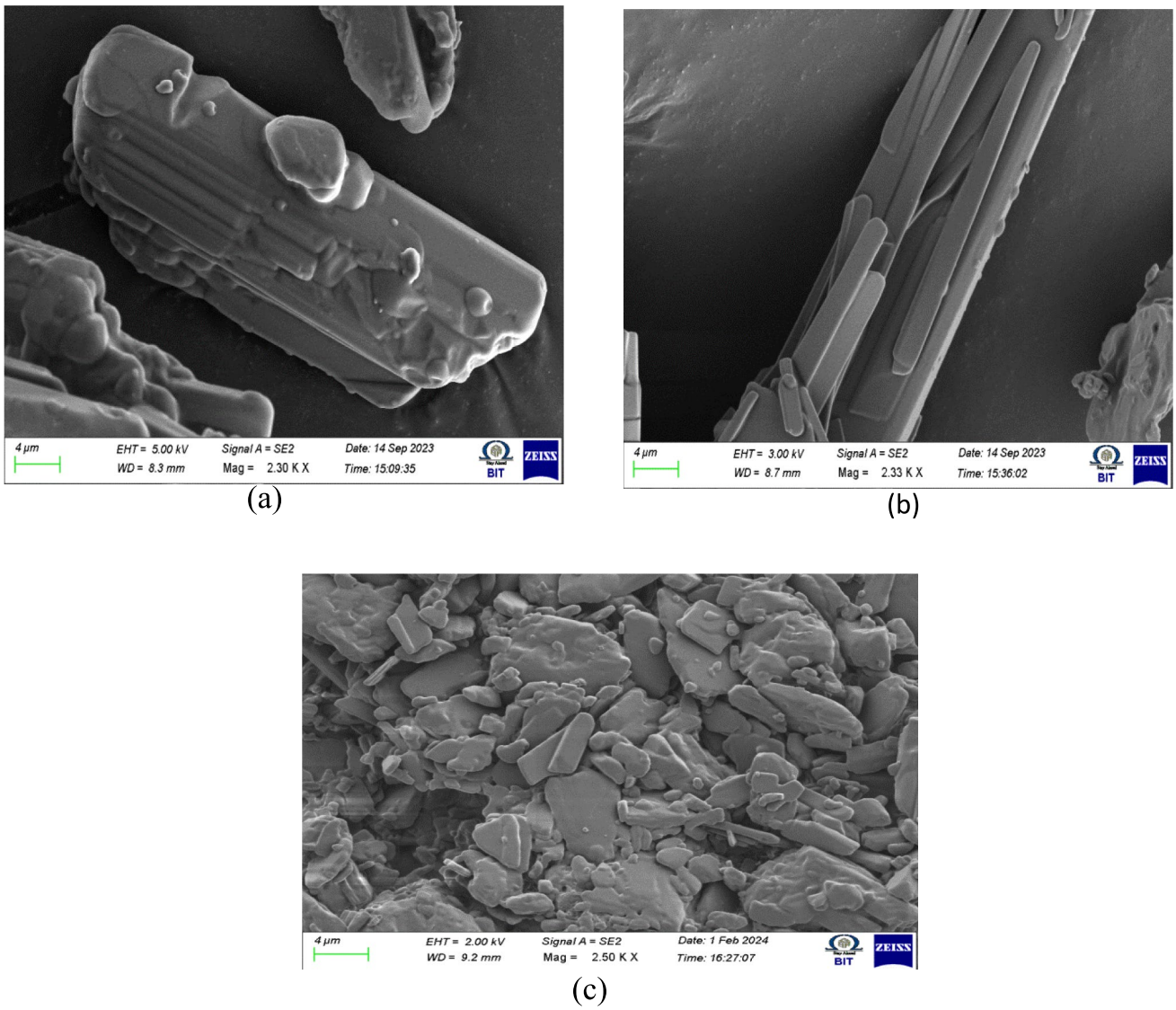

Fig. 1 **a** FESEM image of KGA + 6BAO, **b** FESEM image of KGA + 12BAO, **c** FESEM image of KGA + 6BAO and KGA + 12BAO binary mixture (0.1 *X*/0.9 *Y*)

3.4 Phase Transition Temperature Confirmation: DSC

The thermal properties of the binary mixtures are well understood from the thermograms obtained by DSC for the binary mixtures [41–44]. Phase transition temperatures along with the associated enthalpy values [41] of the individual mesophase are directly obtained from the thermogram, whereas the thermal equilibrium of the system [42], order of transition [31], thermal stability factor [44], and specific heat values [44] are derived from the thermogram data, which enhances the thermal properties of the mesogenic binary mixtures obtained. DSC thermograms are obtained at two different scan rates, viz., 5 °C/min and 10 °C/min, for better investigations. Mesophase transitions are seen through the strong peaks noticed both in heating and cooling runs. The temperature of the phase transition is correlated with POM data, and the phase variance of the binary mixtures is thus confirmed. Based on the occurrence of the transitions in endothermic and exothermic runs, they are classified as monotropic and enantiotropic transitions. Occurrence of a mesophase peak in both runs is termed to be enantiotropic, whereas the availability of a phase transition peak in only one transition is claimed to be monotropic. This has been clearly observed in Table 1. For discussion, the DSC thermogram obtained for KGA + 6BAO and KGA + 12 BAO (0.1 *X*:0.9 *Y*) is shown as Fig. 4, and the exothermic peaks obtained for all five binary mixtures are depicted in Fig. 5. In the endothermic run, three intense peaks are observed that are assigned to crystal to melt transition (93.8

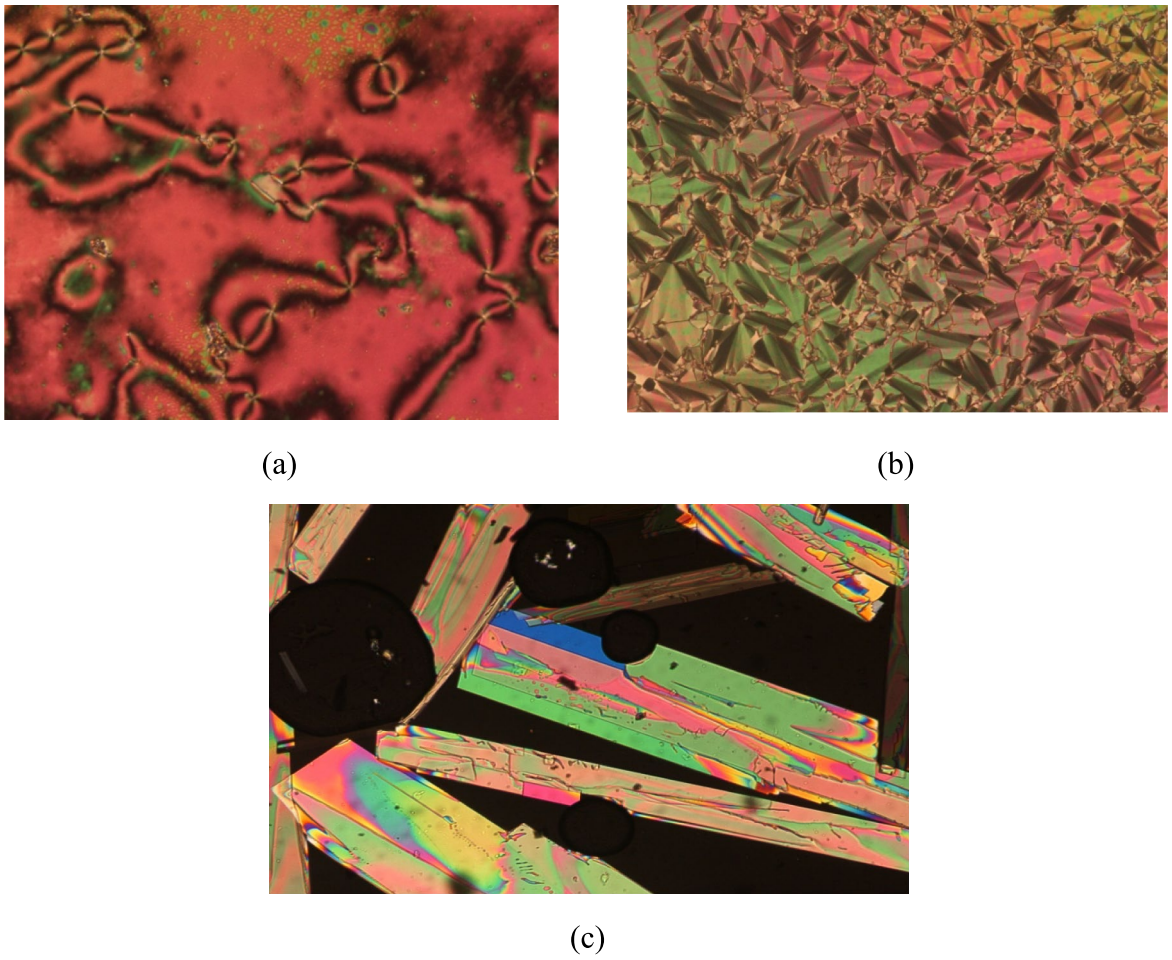

Fig. 2 **a** Threaded nematic texture. **b** Broken focal conic texture of smectic C phase. **c** Smooth mosaic texture of smectic G phase

Table 2 Functional group assessment of KGA + 6BAO and KGA + 12BAO binary mixtures

Molar ratio *X* = KGA + 6BAO *Y* = KGA + 12BAO	$(OH)_{acid}$	$(COOH)_{acid}$
0.1 *X* : 0.9 *Y*	2923	1689
0.3 *X* : 0.7 *Y*	2931	1681
0.5 *X* : 0.5 *Y*	2923	1681
0.7 *X* : 0.3 *Y*	2939	1681
0.9 *X* : 0.1 *Y*	2939	1689

°C/57.92 J g^{-1}) smectic G to smectic C transition (127.6 °C/5.03 J g^{-1}) and smectic C to nematic phase transitions (135 °C/2.96 J g^{-1}), respectively. In the exothermic run of the same binary mixture, four intense peaks are noticed that correspond to isotropic to nematic (132.4 °C/3.54 J g^{-1}), nematic to smectic C (128.5 °C/5.98 J g^{-1}), smectic C to smectic G (119.4 °C/2.24 J g^{-1}), and smectic G to crystal (70.3 °C/18.77 J g^{-1}) phase transitions, respectively. The

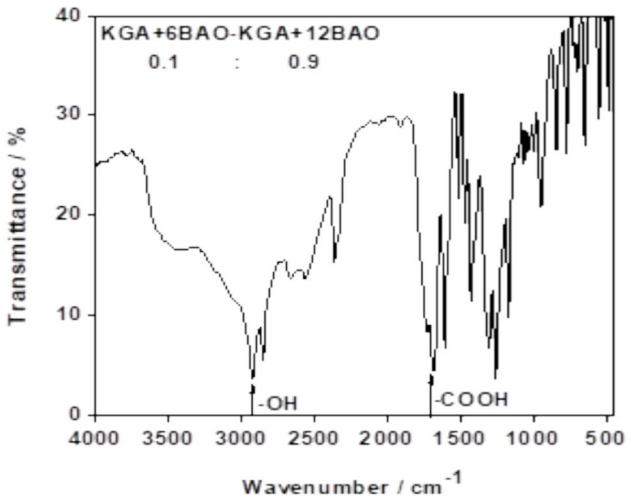

Fig. 3 FTIR spectrum of KGA + 6BAO and KGA + 12BAO binary mixture (0.1 *X*:0.9 *Y*)

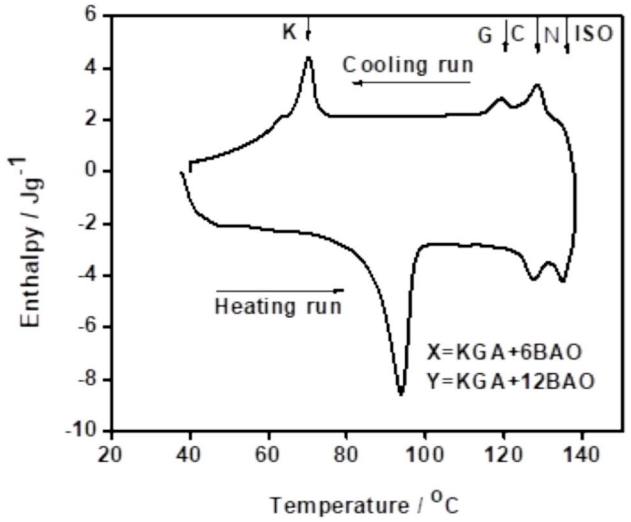

Fig. 4 DSC thermograms of KGA +6BAO and KGA +12BAO binary mixture (0.1 *X*:0.9 *Y*)

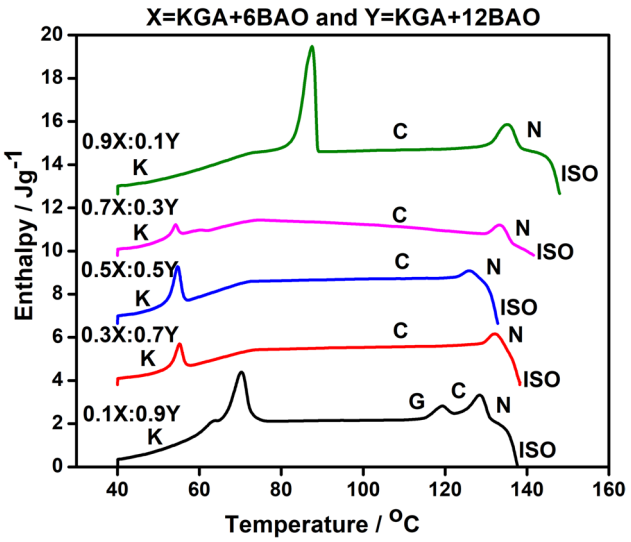

Fig. 5 DSC thermograms obtained for KGA +6BAO and KGA +12BAO binary mixtures in cooling run

phase transition temperatures obtained through POM hold good with the data obtained through DSC, which reflects the chemical and thermal stability of the binary mixtures prepared.

3.5 Phase Diagram

Three mesophases, viz., nematic, smectic C, and smectic G, are observed in the binary mixtures, and the phase variance depends strongly on the concentration of the molar ratio of the precursors used. Figure 6 depicts the phase diagram of the KGA +6BAO and KGA +12 BAO binary mixtures

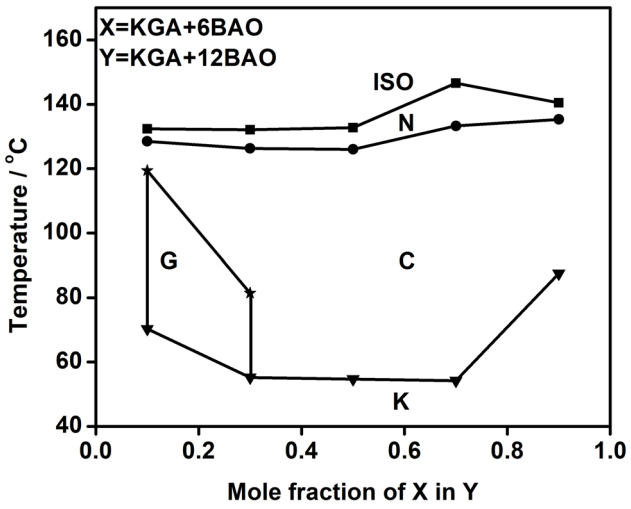

Fig. 6 Phase diagram of KGA +6BAO and KGA +12BAO binary mixtures

prepared. It has been constructed based on the POM and DSC data obtained.

1) Nematic, smectic C, and smectic G are the mesophases that occur in the binary mixtures.
2) Due to the molar ratio influence, the nematic phase prevails throughout the binary mixture, which is not the case in the precursors [31].
3) Similarly, the smectic C mesophase also prevails throughout the binary mixtures.
4) As the molar ratio of KGA +6 BAO dominates, suppression/annihilation of smectic G mesophase is observed.
5) Nematic inducement temperature fairly increases when compared with the precursors, which are attributed to the molar ratio concentration variation of X and Y precursors.
6) Hence, the observation of nematic phase and the enhancement in the thermal span of the same paved the way for the numerous applicational utilities based on this orientational mesophase.

3.6 Energy Equivalence of Binary Mixtures

In order to use the binary mixture for the wide applicational aspect, it is necessary to investigate the energy possessed by the system for better performance [45, 46]. Hence, based on the DSC thermograms obtained for KGA +6BAO and KGA +12 BAO binary mixtures, the energy in and energy out of the system is validated through the thermodynamical law. The internal energy possessed by the binary mixtures in the heating run equals the internal energy possessed by the binary mixtures in the cooling run. Thus, the system remains thermally stable [31]. Enthalpy values possessed by

Table 3 Thermal energy equilibrium possessed by KGA + 6BAO and KGA + 12BAO binary mixtures

Molar ratio *X* = KGA + 6BAO *Y* = KGA + 12BAO	Thermal equilibrium	
	Heating cycle ΔH (J g^{-1})	Cooling cycle ΔC (J g^{-1})
0.1 *X* : 0.9 *Y*	65.91	65.3
0.3 *X* : 0.7 *Y*	25.04	28.17
0.5 *X* : 0.5 *Y*	25.13	20.41
0.7 *X* : 0.3 *Y*	19.06	15.38
0.9 *X* : 0.1 *Y*	41.45	52.31

Table 4 Thermal stability factor for mesophases

Molar ratio *X* = KGA + 6BAO *Y* = KGA + 12BAO	N	C	G
0.1 *X* : 0.9 *Y*	508.76	1127.95	4657.14
0.3 *X* : 0.7 *Y*	749.36	4662.87	1789.46
0.5 *X* : 0.5 *Y*	866.65	6441.96	-
0.7 *X* : 0.3 *Y*	1861.34	7415.63	-
0.9 *X* : 0.1 *Y*	717.08	5324.92	-

the individual phase transitions are cumulated and compared in both heating and cooling runs. Meagre variation in the magnitude of the internal energy is attributed to the nature of the phase transition that occurs in the thermal run. Table 3 portrays the energy equivalence of all the KGA + 6BAO and KGA + 12 BAO binary mixtures.

3.7 Thermal stability factor

Physicochemical investigation includes the analysis of individual mesophase thermal stability also. This thermal stability factor refers to the effectiveness of the mesophase usage for viability [31, 44, 47]. Table 4 reflects the thermal stability factor achieved for all the mesophases observed in KGA + 6BAO and KGA + 12 BAO binary mixtures. The magnitude of the stability is arrived at by considering the thermal range of mesophases and their corresponding onset and offset temperatures observed in the cooling run of the DSC thermograms. The product of the thermal range and the average between the transition temperatures give the thermal stability factor. Data reflected in Table 1 is utilized in obtaining Table 4.

3.8 Analysis of Order of Phase Transition

The properties possessed by the mesophases are also influenced by the order of transition exhibited by them. Various techniques have been adopted by the researchers in

Table 5 Order of phase transition observed in binary mixtures

Molar ratio *X* = KGA + 6BAO *Y* = KGA + 12BAO	Phase variance	Ratio	Order of transition
0.1 *X* : 0.9 *Y*	N	2.08	Second
	C	2.08	Second
	G	2.13	Second
0.3 *X* : 0.7 *Y*	N	1.64	Second
	C	1.80	Second
	G	1.81	Second
0.5 *X* : 0.5 *Y*	N	1.68	Second
	C	1.81	Second
0.7 *X* : 0.3 *Y*	N	0.39	First
	C	0.75	First
0.9 *X* : 0.1 *Y*	N	1.75	Second
	C	1.80	Second

Table 6 Mesogenic occupancy of phase variance in binary mixtures

Molar ratio *X* = KGA + 6BAO *Y* = KGA + 12BAO	Mesogenic range (%)		
	N	C	G
0.1 *X* : 0.9 *Y*	6.3	14.6	79.1
0.3 *X* : 0.7 *Y*	7.5	58.4	34.1
0.5 *X* : 0.5 *Y*	8.6	91.4	-
0.7 *X* : 0.3 *Y*	14.4	85.6	-
0.9 *X* : 0.1 *Y*	9.8	90.2	-

calculating the order of transition, and a popular method that remains valid effectively still is the method followed by Navard and Cox [48]. Either the sample weight or the scan rate

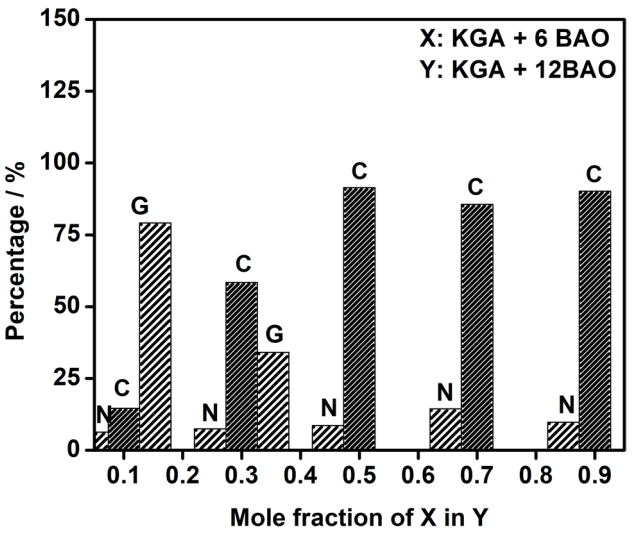

Fig. 7 Mesophase occupancy in KGA + 6BAO and KGA + 12BAO binary mixtures

of the binary mixture should be doubled, and the peak height transition possessed by the mesophase is evaluated and fitted to the equation proposed by Cox. If the magnitude of the transition lies less than $\sqrt{2}$, then the order is confirmed to be first-order transition while if the magnitude is greater than $\sqrt{2}$, then the order is claimed to be second-order transition.

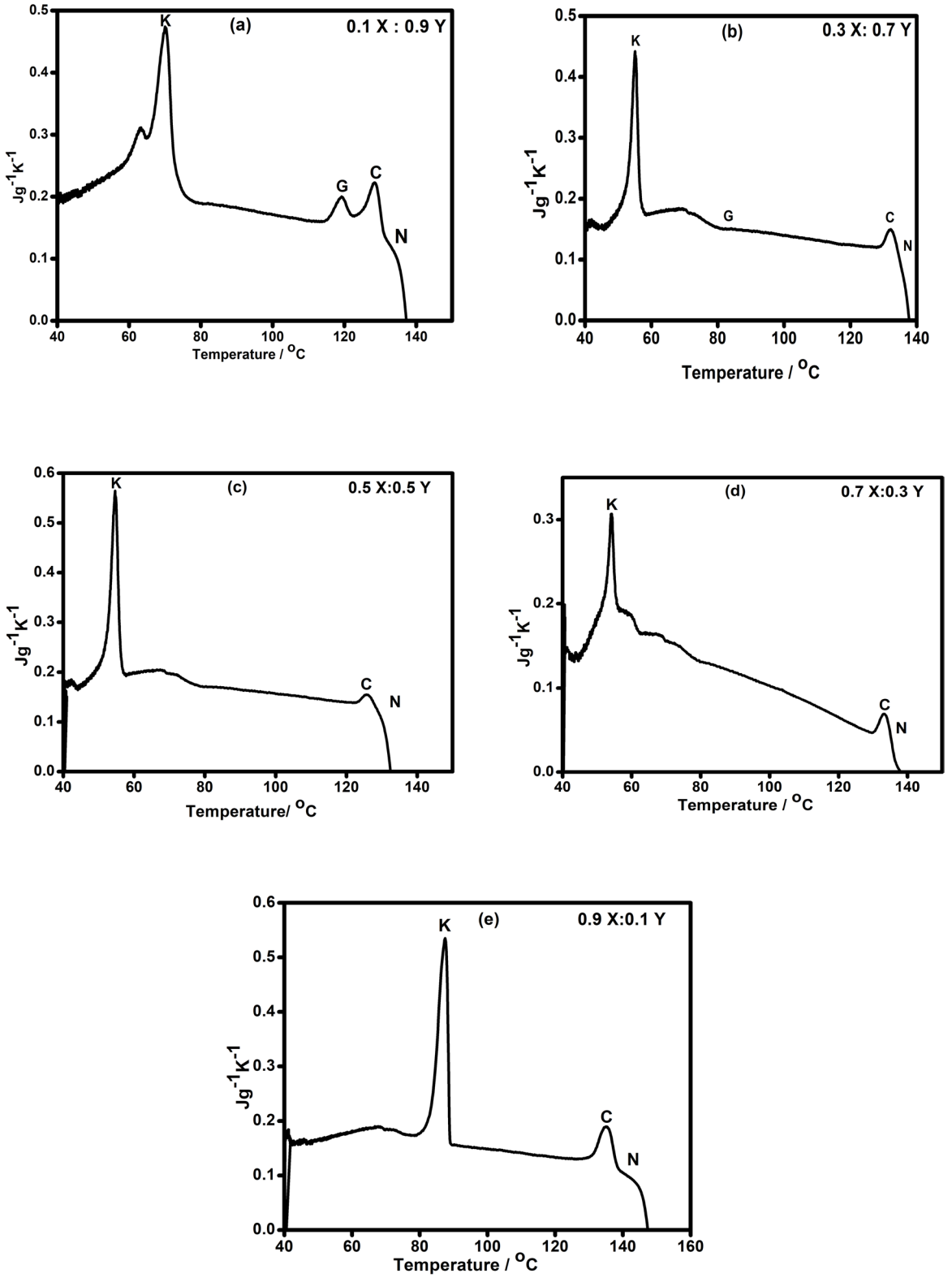

Fig. 8 **a**–**e** Specific heat curves obtained for KGA + 6BAO and KGA + 12BAO binary mixtures

Table 5 consolidates the order of transition possessed by individual mesophases of all the five binary mixtures prepared from KGA + 6BAO and KGA + 12 BAO precursors.

3.9 Mesogenic Range of Binary Mixtures

From the above analysis, it is clearly noticed that the nematic phase prevails throughout the KGA + 6BAO and KGA + 12 BAO binary mixtures irrespective of the phase variance observed in the precursors due to the molar ratio influence. Table 6 reflects the mesogenic range of individual phase transitions in terms of percentage, which elevates the utility of the particular mesophase. A fair magnitude of nematic phase noticed dominates the applicational utility of the prepared binary mixtures. Figure 7 portrays the graphical representation of the mesogenic range observed in the five binary mixtures.

3.10 Specific Heat Capacity of the Binary Mixtures

DSC thermogram data obtained for an empty pan, reference, and the sample are considered for deriving the specific heat capacity [44, 49] of KGA + 6BAO and KGA + 12 BAO binary mixtures. This thermal property affects the thermal utility of the prepared binary mixtures. The ASTM E1269-05.4 method is used in obtaining the specific heat curves of the binary mixtures in the cooling run, which includes the mass of the specimen, sample, and reference; the rate of heating; and the heat flow difference. The specific heat curve obtained is identical to the DSC thermograms, thus validating the method adopted and reflecting the heat capacity possessed by the individual mesophase transition. Figure 8 **a**–**e** reflect the specific heat curves obtained for all five binary mixtures, and the correlation between the DSC thermogram validates the technique and the thermodynamical law.

4 Conclusion

Five binary mixtures are prepared from KGA + 6BAO and KGA + 12BAO precursors whose phase polymorphism has been influenced by molar ratio variation. Physicochemical analysis of the binary mixtures is carried out through different investigations. Surface morphology investigation exhibiting the combination of sheet- and rod-like structures in a uniform manner, which is a token of evidence for the binary mixtures prepared to exhibit uniform optical and thermal properties. Three mesophases, namely, nematic, smectic C, and smectic G, are observed in the POM analysis. Confirmation of intermolecular complementary hydrogen bonding and the formation of mesogenic complex upon complexation is the fundamental chemical characterization carried out through FTIR analysis. In the endothermic run, three intense peaks are observed that are assigned to crystal to melt transition, smectic G to smectic C transition, and smectic C to nematic phase transition, respectively. In the exothermic run of the same binary mixture, four intense peaks are noticed that correspond to isotropic to nematic, nematic to smectic C, smectic C to smectic G, and smectic G to crystal phase transitions, respectively, obtained through DSC, which reflects the chemical and thermal stability of the binary mixtures. Nematic phase prevails throughout the series, which is not the case in precursors.

Acknowledgements The infrastructural support provided by Centre for Research, Bannari Amman Institute of Technology, is gratefully acknowledged.

Author Contributions J. Vivekanandan, N. Pongali sathya prabu, wrote the main manuscript text and prepared figures. N. Pongali sathya prabu & Sang Yeol Lee reviewed the manuscript.

Funding No funds, grants, or other support was received.

Data Availability No datasets were generated or analysed during the current study.

Declarations

Use of Artificial Intelligence (AI) Tools The authors declare they have not used AI tools in the creation of this article.

Competing Interests The authors declare no competing interests.

References

1. H. Fujikake, H. Sato, T. Murashige, Displays (2004). https://doi.org/10.1016/j.displa.2004.04.001
2. J.P.F. Lagerwall, Giusy Scalia. Curr. Appl. Phys. (2012). https://doi.org/10.1016/j.cap.2012.03.019
3. Antonio d Alessandro, Rita Asquini, Appl Sci. (2021) https://doi.org/10.3390/app11188713
4. X. Li et al., Liq. Cryst. **43**(7), 955 (2016). https://doi.org/10.1080/02678292.2016.1153732
5. R.B. Alnoman, M. Hagar, H.A. Ahmed, M.M. Naoum, H.A. Sobaih, J.S. Almshaly, M.M. Haddad, R.A. Alhaisoni, T.A. Alsobhi, Crystals (2020). https://doi.org/10.3390/cryst10040319
6. A. Ghanadzadeh Gilani, N. Khoshroo, M. Mohammadi, P. Kula, N. Rychłowicz, J Mol Liq. (2023) https://doi.org/10.1016/j.molliq.2022.120925
7. L.A. Serrano, M.J. Fornerod, Ye. Yang, S. Gaisford, F. Stellacci, S. Guldin, Soft Matter (2018). https://doi.org/10.1039/C8SM00327K
8. V. Thangavel, B. Venkataraman, S. Prakasan, J. Ramasamy, Vijayakumar Vellalapalayam Nallagounder. Braz. J. Phys. (2019). https://doi.org/10.1007/s13538-019-00724-y
9. S.Z. Mohamady, R.I. Nessim, O.R. Shehab, M.M. Naoum, Mol. Cryst. Liq. Cryst. (2006). https://doi.org/10.1080/15421409096007 2
10. M.M. Naoum, S.Z. Mohammady, H.A. Ahmed, Liq. Cryst. (2010). https://doi.org/10.1080/02678292.2010.497228

11. M.M. Naoum, A.A. Fahmi, M.A. Alaasar, M.E. Abdel-Aziz, Liq. Cryst. (2011). https://doi.org/10.1080/02678292.2010.550069
12. H.A. Ahmed, M.M. Naoum, G.R. Saad, Liq. Cryst. (2013). https://doi.org/10.1080/02678292.2013.788739
13. H.A. Ahmed, M.M. Naoum, Thermochim. Acta (2014). https://doi.org/10.1016/j.tca.2013.10.027
14. H.A. Ahmed, M.M. Naoum, G.R. Saad, Liq. Cryst. (2016). https://doi.org/10.1080/02678292.2016.1166528
15. H.A. Ahmed, Liq. Cryst. (2015). https://doi.org/10.1080/02678292.2014.963181
16. T. Kato, Science (2002). https://doi.org/10.1126/science.1070967-a
17. W. Li, J. Zhang, B. Li, M. Zhang, Wu. Lixin, Chem. Commun. (2009). https://doi.org/10.1039/B909605A
18. D. Cupelli, Fiore Pasquale Nicoletta, Sabrina Manfredi, Marco Vivacqua, Patrizia Formoso, Giovanni De Filpo, Giuseppe Chidichimo. Sol. Energy Mater. Sol. Cells (2009). https://doi.org/10.1016/j.solmat.2009.08.002
19. F.P. Nicoletta, D. Cupelli, G. De Filpo, M. Macchione, G. Chidichimo, Appl. Phys. Lett. (2000). https://doi.org/10.1063/1.1330223
20. D. Cupelli, F.P. Nicoletta, G. De Filpo, P. Formoso, G. Chidichimo, J Polym Sci. Part B: Polym Phys. (2011). https://doi.org/10.1002/polb.22184
21. S. Kannan, A. Sekar, K. Sivaperuman, J. Mater. Chem. C. (2020). https://doi.org/10.1039/d0tc04260a
22. A. Arunkumar, P. Ramasamy, J. Cryst. Growth (2014). https://doi.org/10.1016/j.jcrysgro.2013.10.005
23. M. Karimi-Jafari, L. Padrela, G.M. Walker, D.M. Croker, Cryst. Growth Des. (2018). https://doi.org/10.1021/acs.cgd.8b00933
24. M.A.E. Yousef, V.R. Vangala, Cryst. Growth Des. (2019). https://doi.org/10.1021/acs.cgd.8b01898
25. Y. Qi, Y. Liu, X. Li, Xu. Juan, Qi. Zhang, Cryst. Eng Comm. (2025). https://doi.org/10.1039/D4CE01171F
26. Takashi Kato, Jean M. J. Frechet, J Am Chem Soc. (1989) https://doi.org/10.1021/ja00204a044
27. Seung Koo Kang, Edward T. Samulski, Liq Cryst. (2000) https://doi.org/10.1080/026782900202822
28. G. Chandrasekar, N. Pongali Sathya Prabu, M. L. N. Madhu Mohan, Ferroelectrics (2018) https://doi.org/10.1080/00150193.2018.1432744
29. G. Sangameswari, N. Pongali Sathya Prabu, M. L. N. Madhu Mohan, Phase Transit. (2015) https://doi.org/10.1080/01411594.2015.1039011
30. N. Pongali Sathya Prabu, M. L. N. Madhu Mohan, J Therm Anal Calorim. (2013) https://doi.org/10.1007/s10973-012-2812-6
31. K.S.Usha, P. Rohini, J. Vivekanandan, N. Pongali Sathya Prabu, M. L. N. Madhu Mohan, Mol Cryst Liq Cryst. (2023) https://doi.org/10.1080/15421406.2022.2102749
32. Takashi Kato, Jean M. J. Frechet, Paul G. Wilson, Takeshi Saito, Toshiyuki Uryu, Akira Fujishima, Chihiro Jin, Fumiko Kaneuchi, Chem Mater. (1993) https://doi.org/10.1021/cm00032a012
33. N. Pongali Sathya Prabu, M. L. N. Madhu Mohan, Kaushik Pal, J Mol Liq. (2021) https://doi.org/10.1016/j.molliq.2021.117386
34. M.L.N. Madhu Mohan, N. Pongali Sathya Prabu, Kaushik Pal, Materials Letters (2021) https://doi.org/10.1016/j.matlet.2021.130821
35. P. Rohini, M.L.N. Madhu Mohan, N. Pongali Sathya Prabu, Optik (2022) https://doi.org/10.1016/j.ijleo.2022.168951
36. V.G.W. Gray, J. W. Goodby, Smectic Liquid Crystals: Textures and Structures (Leonard Hill, Glasgow, 1984).
37. C. Kavitha, N. Pongali Sathya Prabu, K. Sankarra Narayanan, M.L.N. Madhu Mohan, Ferroelectrics (2023) https://doi.org/10.1080/00150193.2023.2243561
38. G. Chandrasekar, N. Pongali Sathya Prabu, M.L.N. Madhu Mohan, Mol Cryst Liq Cryst. (2017) https://doi.org/10.1080/10807039.2017.1357394
39. N. Pongali Sathya Prabu, M.L.N. Madhu Mohan, Mol Cryst Liq Cryst. (2016) https://doi.org/10.1080/15421406.2016.1149019
40. K. Karthika, C. Senthilkumar, K.S. Dhivya, M. Srinivasan, P. Srinivasan, J. Mater. Sci. Mater. Electron. (2023). https://doi.org/10.1007/s10854-023-11061-x
41. N. Pongali Sathya Prabu, D.M. Potukuchi, M.L.N. Madhu Mohan, Physica B Con Mat. (2012) https://doi.org/10.1016/j.physb.2012.05.029
42. P. Rohini, N. Pongali Sathya Prabu, M.L.N. Madhu Mohan, Mol Cryst Liq Cryst (2016) https://doi.org/10.1080/15421406.2016.1149022
43. A. J. Gopunath, T. Chitravel, C. Kavitha, N. Pongali Sathya Prabu, M. L. N. Madhu Mohan, Mol Cryst Liq Cryst. (2014) https://doi.org/10.1080/15421406.2013.839315
44. G. Sangameswari, N. Pongali Sathya Prabu, M. L. N. Madhu Mohan, J Therm Anal Calorim. (2017) https://doi.org/10.1007/s10973-016-5925-5
45. M.B. Sied, S. Diez, J. Salud, D.O. López, P. Cusmin, J. Ll, Tamarit, María Barrio. J. Phys. Chem. B (2005). https://doi.org/10.1021/jp051957x
46. B. Robles-Hernández, N. Sebastián, J. Salud, S. Diez-Berart, D. A. Dunmur, G. R. Luckhurst, D. O. López, M. R. de la Fuente, Phys Rev. E (2016) https://doi.org/10.1103/PhysRevE.93.062705
47. N. Meera Mohideen, V. N. Vijayakumar, P. Valarmathi, Mol. Cryst. Liq. Cryst. (2025) https://doi.org/10.1080/15421406.2024.2443259
48. P. Navard, R. Cox, Mol. Cryst. Liq. Cryst. (1984). https://doi.org/10.1080/01406568408070538
49. K.J. Lushington, G.B. Kasting, C.W. Garland, Phys. Rev. B (1980). https://doi.org/10.1103/PhysRevB.22.2569